



Full paper



Multifunctional meta-tribomaterial nanogenerators for energy harvesting and active sensing

Kaveh Barri^{a,1}, Pengcheng Jiao^{b,c,1}, Qianyun Zhang^{a,1}, Jun Chen^d, Zhong Lin Wang^{e,f,*}, Amir H. Alavi^{a,g,h,**,2}

^a Department of Civil and Environmental Engineering, University of Pittsburgh, Pittsburgh, PA, USA

^b Institute of Port, Coastal and Offshore Engineering, Ocean College, Zhejiang University, Zhoushan, Zhejiang, China

^c Engineering Research Center of Oceanic Sensing Technology and Equipment, Zhejiang University, Ministry of Education, China

^d Petersen Institute of NanoScience and Engineering, University of Pittsburgh, Pittsburgh, PA, USA

^e School of Materials Science and Engineering, Georgia Institute of Technology, Atlanta, GA, USA

^f Beijing Institute of Nanoenergy and Nanosystems, Beijing 101400, China

^g Department of Bioengineering, University of Pittsburgh, Pittsburgh, PA, USA

^h Department of Computer Science and Information Engineering, Asia University, Taichung, Taiwan

ARTICLE INFO

Keywords:

Metamaterial
Multifunctional material
Triboelectric nanogenerators
Energy harvesting
Sensors

ABSTRACT

Discovering novel multifunctional metamaterials with energy harvesting and sensing functionalities is likely to be the next technological evolution of the metamaterial science. Here, we introduce a novel concept called self-aware composite mechanical metamaterial (SCMM) that can transform mechanical metamaterials into nanogenerators and active sensing mediums. In pursuit of this goal, we examine new paradigms where finely tailored and seamlessly integrated self-recovering snapping microstructures composed of topologically different triboelectric materials can form self-powering and self-sensing meta-tribomaterial systems. We explore various deformation mechanisms required to induce contact electrification between these snapping microstructures under periodic deformations. The multifunctional meta-tribomaterial systems created under the SCMM concept will act as triboelectric nanogenerators capable of generating electrical signals in response to the applied mechanical excitations. The generated electrical signal can be used for active sensing of the applied force and can be stored for empowering sensors and embedded electronics. We conduct theoretical and experimental studies to understand the mechanical and electrical behavior of the multifunctional SCMM systems. The broad application of the proposed SCMM concept for designing artificial materials with novel properties and functionalities is highlighted via prototyping self-powering and self-sensing blood vessel stents and shock absorbers.

1. Introduction

One of the obstacles that is limiting the development of deployable integrated sensing and actuation solutions in multifunctional systems is the scarcity of power. Many applications require the use of miniaturized low-powered sensing and actuation systems. In spite of the significant developments in the area of localized sensing and actuation [1,2], most of the developed systems to date still rely on batteries thus limiting the lifetime of the device as well as the diagnosis possibilities. Thus, energy harvesting has been a topic given great attention in recent years as a

viable alternative [3]. The key parameter of any energy harvesting device is its conversion efficiency that depends strongly on the conversion medium. In the past, natural materials were often chosen as conversion media for different energy harvesting devices. However, the conversion efficiency is limited by the properties of natural material and structures. To address these issues, metamaterials have been introduced for energy harvesting in recent years [4]. Metamaterials with non-traditional physical behaviors provide innovative mechanisms for energy harvesting. A survey of the literature reveals that metamaterials used for energy harvesting mainly include electromagnetic metamaterials, photonic

* Corresponding author at: School of Materials Science and Engineering, Georgia Institute of Technology, Atlanta, GA, USA.

** Corresponding author at: Department of Civil and Environmental Engineering, University of Pittsburgh, Pittsburgh, PA, USA.

E-mail addresses: zhong.wang@mse.gatech.edu (Z.L. Wang), alavi@pitt.edu (A.H. Alavi).

¹ Authors contributed equally to this work.

² <https://www.engineering.pitt.edu/amirhosseinalavi/>

crystals and acoustic metamaterials [5,6]. As architected, structural materials comprised of engineered microstructures, mechanical metamaterials are fairly new branch of metamaterial systems that have marked their debut during the last few years [7–9]. Mechanical metamaterials have inspired the popularity of research on advanced materials with extraordinary properties [10–12]. The unusual mechanical properties often include either negative properties or extreme properties. Examples of negative properties are negative Poisson's ratio [13, 14], negative thermal expansion coefficient [12], negative compressibility [11], and negative stiffness [15,16]. Extremely high stiffness to mass ratio [17], and extremely high (low) resistance against deformation in specific directions [18] are examples of the extreme properties. The mechanical metamaterial concept is appealing in its potential to accelerate the materials discovery and development by satisfying the requirements of specific and desired mechanical properties. Research efforts have been dedicated to exploring the performance of mechanical metamaterial and obtaining superior mechanical properties using the structure strategy [19–21].

Studies have been particularly carried out on 2D layout and 3D form structures that are maintained uniform in the thickness direction [13, 22]. Negative Poisson ratio has been reported from those structures due to the embedded hole-like designs. Recent interest has been shifted to utilize multifunctional mechanical metamaterial in devices and techniques in energy absorption, artificial muscles, drug delivery, and soft robots [23]. However, a substantial portion of the current effort in the arena of multifunctional mechanical metamaterials has been merely going into exploring new geometrical design of micro/nano-architectures to improve or identify unusual sets of mechanical properties [23]. There is a critical shortage in research needed to engineer new aspects of functionalities into the texture of mechanical metamaterials for multifunctional applications. In particular, introducing the self-powering and self-sensing functionality into the material design could in theory lay the foundation for living engineered materials and structures that can empower, sense and program themselves. Despite its capacity to open new horizons for mechanical metamaterials, the entire concept of mechanical metamaterials for energy harvesting is still in its infancy. The limited studies in this arena are merely based on attaching external energy harvesting transducers to the structural frame of the metamaterial to convert its localized deformations into electric energy [8,24,25]. A major issue with such segregated designs is that added mass and increased drag due to attaching an external energy harvesting transducer will significantly degrade the structural performance of the mechanical metamaterial system. Yet, a major challenge ahead is how to develop mechanical metamaterial systems that can utilize their entire constituent components as an energy harvesting medium for self-powering or local powering of sensing and actuating devices.

Here, we aim to advance the knowledge and technology required to create a new class of multifunctional mechanical metamaterial systems with energy harvesting functionality. The meta-tribomaterial systems created under the proposed self-aware composite mechanical metamaterial (SCMM) concept are composed of finely tailored and topologically different triboelectric microstructures. The beauty of the concept is that the entire meta-tribomaterial structure serves as a triboelectric nanogenerator (TENG) as well as an active sensing medium to directly collect information about its operating environment. This has not been possible with any competing mechanical metamaterial technologies so far. A meta-tribomaterial naturally inherits the enhanced mechanical properties offered by classical mechanical metamaterials. Furthermore, a practical aspect of the SCMM concept is that it enables designing layered composite systems using a wide range of the organic and inorganic materials from the triboelectric series. Theoretical and experimental studies are conducted to understand the mechanical and electrical behavior of the composite mechanical meta-tribomaterials designed according to the SCMM concept. Thereafter, we demonstrate the feasibility of integrating the SCMM mechanisms to design

multifunctional systems for real-life engineering applications such as self-sensing and self-powering cardiovascular stents and shock absorbers.

2. Results and discussion

The quest for a truly multifunctional mechanical metamaterial with energy harvesting, sensing and programmability has been the Holy Grail for material scientists. SCMM is a new generation of composite mechanical metamaterials offering self-powering and self-sensing functionalities along with the boosted mechanical properties. The idea behind developing any SCMM system is that finely tailored and seamlessly integrated microstructures composed of topologically different triboelectric materials can form a hybrid meta-tribomaterial system with active energy harvesting and sensing functionalities. On the other hand, a composite mechanical metamaterial composed of different materials that are organized in a periodic manner would potentially boost the mechanical properties such as strength and stiffness [26]. Fig. 1 illustrates our vision for the proposed research study, where architecture tailoring of triboelectric materials via additive manufacturing could form a new class of multifunctional mechanical metamaterials for a broad range of applications (Fig. 1b). Deformation mode of the fabricated microstructures should be engineered through a unique design so that contact electrification will occur between the two surfaces as the SCMM structure undergoes periodic deformations due to mechanical excitations. The SCMM contacting/sliding surfaces act as conductive and dielectric layers similar to a TENG as shown in Fig. 1a. Due to the contact electrification, the conductive and dielectric layers accumulate positive and negative charges, respectively. As the SCMM structure is unloaded, the transferred charge remains on the dielectric surface. This forms a static electric field and a potential difference between the conductive layers. By increasing the loading amplitude, more conductive and dielectric layers of the SCMM matrix engage in the contact–separation process, which results in generating higher electrical output. The electrical output signals can be used for active sensing of the external mechanical excitation applied to the SCMM structure. On the other hand, the generated electrical energy can be harvested and stored to empower sensors and electronics at low power.

From an energy harvesting perspective, the SCMM approach offers new mechanisms for materials and structures that utilize the energy that develops within them (strain and kinetic energy) for a wide range of applications. Incorporating the triboelectric materials as a constituent material into the texture of mechanical metamaterials would expand the useable range of these materials as power harvesters. A nanogenerator SCMM would naturally inherit the outstanding features of the TENGs. It uses neither magnets nor coils; it is light in mass, low in density, low in cost, highly scalable, and it can be fabricated using inorganic and “most of the organic” materials. TENGs have shown a significantly higher power density in comparison with other competitive technologies such as piezoelectric materials and electromagnetic generators [27–29]. The metamaterial “Tree of Knowledge” reveals that sensor applications are one of the pillars of the metamaterials future research [30]. So far, there are very few studies with focus on developing mechanical metamaterial sensors [31,32]. These studies do not use the mechanical metamaterial structure as a sensing medium. Instead, they deploy the mechanical metamaterial simply as a frame that carries active sensing materials (e. g., conductive carbon nanotube (CNT) or graphene-based microstructure layers) to transform the mechanical stimuli into readable electrical signals. From a sensing perspective, introducing the self-sensing functionality into the mechanical metamaterial design via the SCMM concept could in theory lay the foundations for living structures that respond to their environment and self-monitor their condition. In addition to its self-sensing features, an SCMM system is intrinsically sensitive to the applied stresses, and therefore, it can be implemented as a sensor in various materials or structural systems. From a mechanical perspective, SCMMs are composed of different materials that are

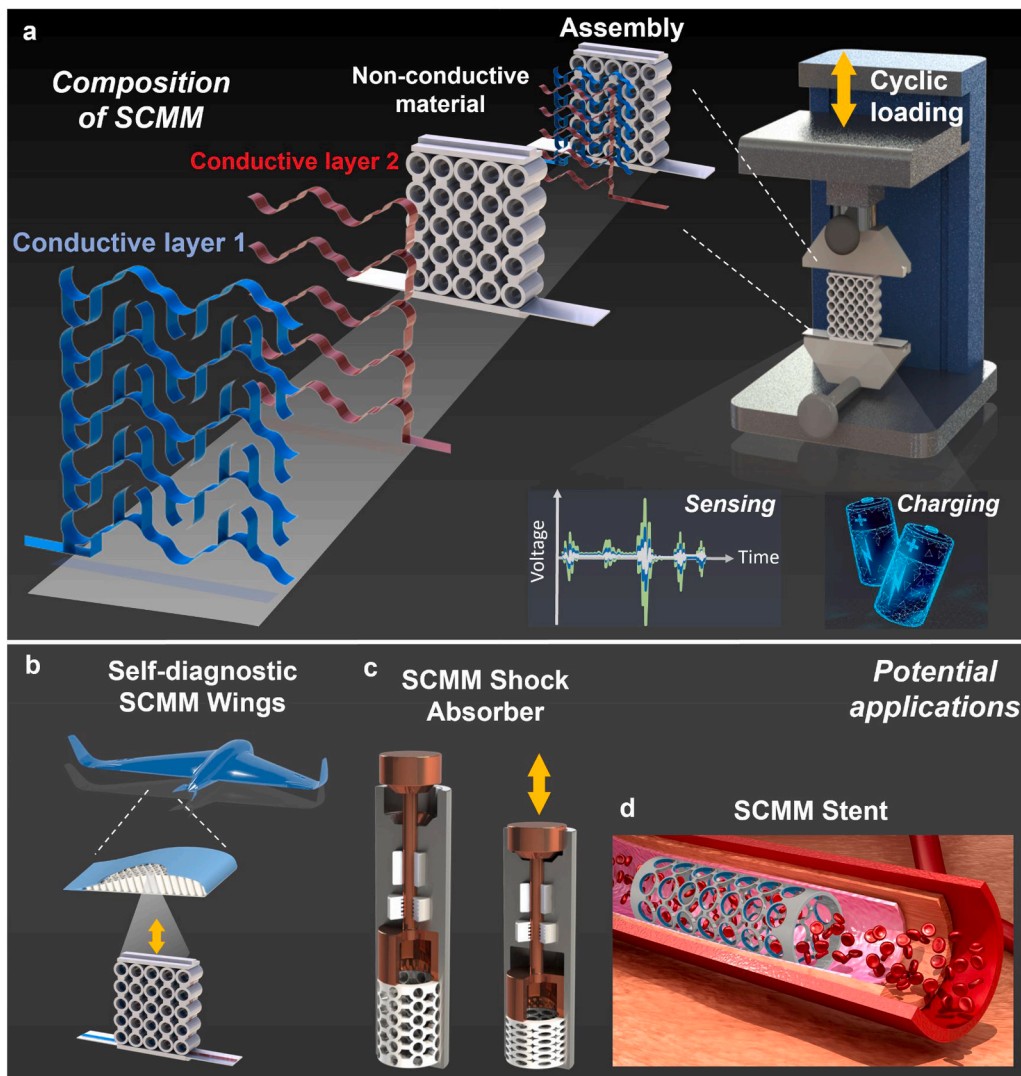


Fig. 1. Vision of the proposed multi-functional meta-tribomaterial concept for energy harvesting and active sensing. a, Composition of a snapping mechanical meta-tribomaterial designed based on the SCMM concept. Broad applications of the proposed concept including: b, A flying wing aircraft with self-diagnostic and energy harvesting wings made of a network of SCMM structures. c, Self-sensing SCMM shock absorber with energy harvesting capabilities. d, Self-powered and self-sensing cardiovascular SCMM stent for continuous monitoring of the artery radial pressure changes due to tissue overgrowth. The stent equipped with a miniaturized wireless interface self-powers itself by harvesting the energy from the arterial pulsations of the blood vessels.

organized in a periodic manner. Therefore, SCMMs not only inherit all features of classical mechanical metamaterials, but could also offer significantly boosted mechanical properties due to their composite structure by overcoming the “rule of mixtures” [26,33].

However, *without loss of generality*, we illustrate this paradigm shift by focusing on the design principles for composite mechanical meta-tribomaterial structures with parallel snapping curved segments. The self-recovering behavior of this type of mechanical metamaterials makes it an ideal case study for the contact-separation mode of triboelectric energy harvesting. Arguably, the proposed concept can be applied to a wide range of other material and metamaterial systems with different geometrical designs and self-recovering behavior. In our study, the metamaterial was made up of multiple bi-stable unit cells. The unit cell consisted of thick horizontal and vertical elements and a thin curved part. The reported structural design is conceptually different from kirigami and serpentine patterns due to the following two reasons: First, kirigami structures (e.g., kirigami metamaterials) are typically reported with transverse deformation caused by cut-induced design. This is while, the SCMM systems have not been observed with transverse deformation under cyclic loading. Secondly, serpentine structures are typically asymmetric in loading direction such as in sinusoidal design. Conversely, an SCMM system is periodically symmetric and thus it evenly deforms in the loading direction. However, in order to incorporate the sensing and energy harvesting features into the metamaterial

functionality, we introduced the TENG concept into its architecture design. The design process is shown in Fig. 2. The electrical output of the designed snapping SCMM is presented in Fig. 3. In order to fabricate the 2D structure of the snapping composite mechanical metamaterial, three constituent layers were defined. The first two layers were conductive layers created as periodic repeatable segments (Fig. 2a and b). The conductive layers were first aligned to act as opposite electrodes. Then, they were embedded inside a thicker dielectric layer serving as the skeleton of the mechanical metamaterial (Fig. 2b). As seen in Fig. 2b, the entire snapping composite mechanical metamaterial structure forms composite matrix composed of the conductive and dielectric layers in a periodic manner. The semicircular-shaped snapping segments include both conductive and dielectric layers. The semicircular-shaped snapping segments were centrally clamped by relatively thicker (stiffer) supporting segments with a connection platform, as illustrated in Fig. 2b. The curved elements were specifically designed in mathematical/trigonometric function form to achieve smooth snap-through transition and symmetrical stable configurations before and after large deformation. The clamped conditions of the snapping beams at both ends were released and connected to supporting segments to create periodic repeatable unit cells and provide local support to prevent lateral displacement and bending at the ends of the semicircular-shaped slender elements. The SCMM was designed to be triggered under cyclic loading in compression with a built-in TENG system activated in a contact-

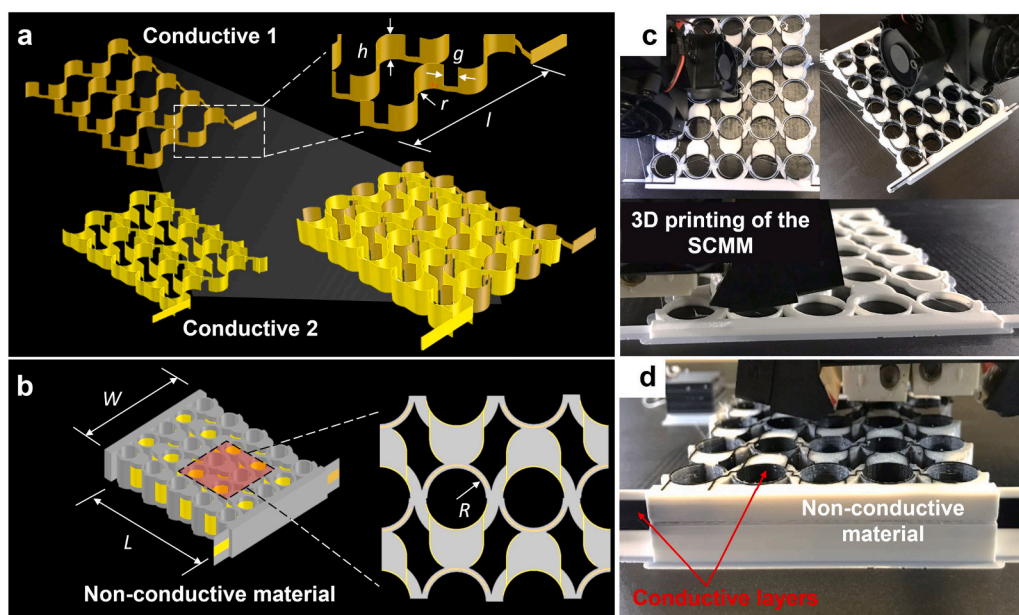


Fig. 2. Designing a 2D mechanical meta-tribomaterial with parallel semicircular-shaped snapping segments according to the SCMM concept. a, the segments of the two conductive layers (Conductive 1 and 2) created as 5 periodic repeatable segments, and the aligned conductive layers. b, The schematic representation of the composite matrix composed of the conductive and non-conductive layers in a periodic manner. c and d 3D printing of the SCMM prototypes composed of the conductive and non-conductive layers that are involved in the contact–separation process.

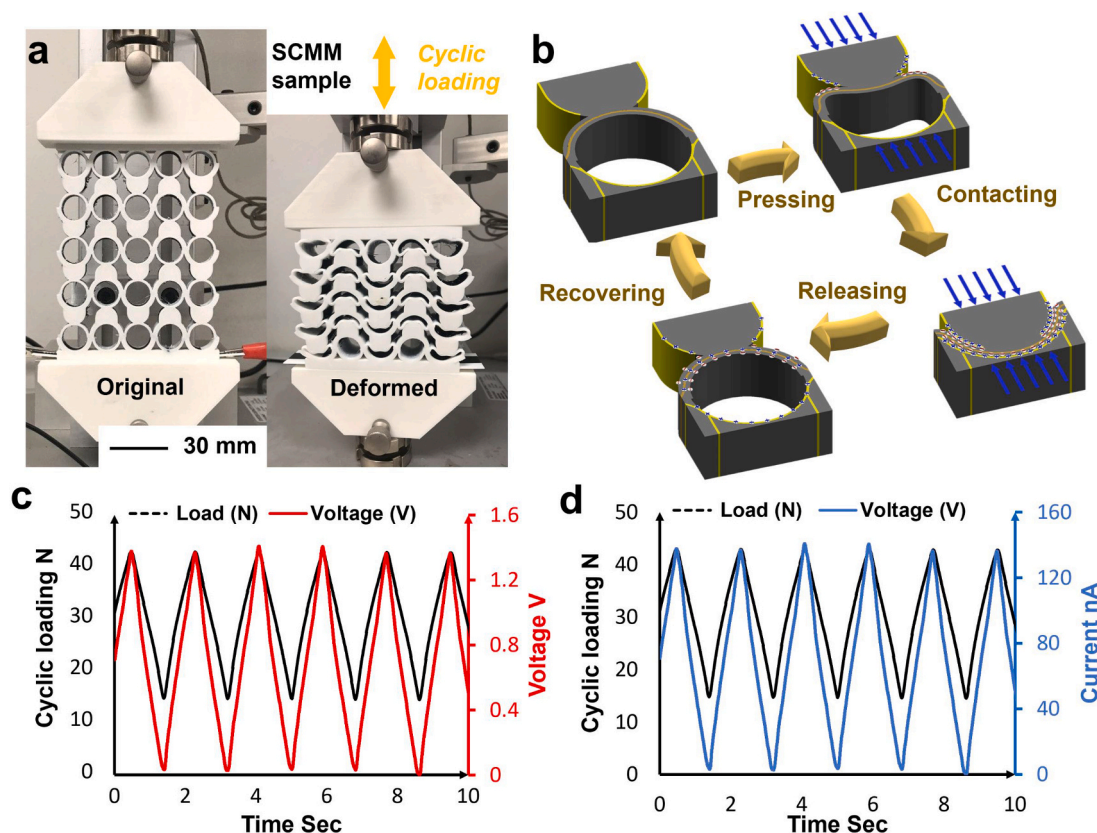


Fig. 3. A self-sensing and self-charging 2D mechanical meta-tribomaterial. a, 3D printed SCMM sample comprised of 5×5 unit cells at the original and deformed states under cyclic loading. b, Snapping mechanisms of the elastic bulking semicircular-shaped snapping shells, and the operating principle of the SCMM unit cells in the contact-separation mode TENG. Applied cyclic loading and the corresponding c voltage and d current generated by the proposed SCMM (in red and blue, respectively).

separation mode. In order to fabricate this complex design as one integrated unit, a dual extruder 3D printer was used that could support printing with a variety of multi-material filaments. There is a wide range of organic and inorganic materials from the triboelectric series that can be used to fabricate the conductive and dielectric layers. We purposely

chose materials with a large difference in triboelectric polarity to maximize the electrification between the two layers. Polylactic Acid (PLA) with carbon black (Young's modulus $E = 3000$ MPa, Poisson's ratio $\nu = 0.48$) and Thermoplastic Polyurethane (TPU) ($E = 12$ MPa, $\nu = 0.25$) were used as the conductive and dielectric layers, respectively.

In Fig. 2a and b, h , g , l , L , W , and R are 15.5 mm, 6.5 mm, 82.6 mm, 119.35 mm, 100 mm, and 7.76 mm, respectively. The thicknesses of the conductive and non-conductive layers are 0.65 mm and 0.3 mm, respectively. The detailed device fabrication process is described in Section 4.

Fig. 3 presents the testing results of the composite snapping mechanical meta-tribomaterial designed according to the SCMM concept. Uniaxial loading experiments were performed on the 3D printed metamaterial specimen. Cycling loading at 0.5 Hz frequency was applied to the specimen under displacement control until it was fully compacted. The displacement range was controlled to be between 5 mm and 10 mm. The applied load changed between 15 N and 45 N. Under uniaxial loading, the sample undergoes a large deformation caused by stiffness mismatch between snapping (buckling instabilities) and supporting (relatively stiffer/thicker) components, exhibiting very small transverse deformation after every snapping. Based on the multi-stable/self-recovering mechanism, phase transformation/shape-reconfiguration and zero (or close to zero) Poisson's ratio can be achieved up to large morphological change (Fig. 3a). As shown in Fig. 3b, when a normal vertical force applied in the middle of the curved beams, the semicircular-shaped segment is mechanically deformed (buckled), snapping from first/original stable state (State I) to fully compacted/deformed stable state (State III) at a critical applied force. In a very ideal situation, the constrained conditions at both ends are strong and the two stable states are symmetric, the reaction force will be symmetric from one to the other stable state under displacement control which means that an identical reverse force is needed that allows the deformed beams to return to their original configuration. In the case of a self-recovering

snapping, the constant positive force means that the fully compacted segments (State III) automatically return to their initial stable configuration (State I) after the load is removed. Under compressive loads, the snapping mechanical metamaterial structure undergoes periodic deformations and contact electrification occurs between the conductive and non-conductive surfaces. By unloading the structure, a potential difference is formed between the conductive layers. Higher loading amplitude results in larger deformations. Consequently, more conductive and dielectric layers of the matrix get involved in the contact-separation process. This leads to higher rate of the electrostatically-induced electron transfer and generating higher voltage.

In order to record the voltage generated due to the applied mechanical excitations, wires were connected to the extended parts of the conductive layers, as shown in Fig. 3a. The voltage values were read using a National Instruments 9220 DAQ module with 1 G Ω impedance. The applied cyclic loads and the corresponding voltage and current generated by the proposed mechanical metamaterial structure are shown in Fig. 3c and d. As seen, the voltage is proportional to the applied force. Fig. 4 illustrates the SCMM charging characteristics under periodic mechanical motion. Fig. 3a and b shows the voltage-time and the stored charge-time relationships at different load capacitances, respectively. As seen in Fig. 3a, the capacitors are charged at the maximum speed at $t = 0$. Thereafter, the speed of charging decreases gradually until it reaches the saturation voltage. The saturation voltage is about 0.85 V, which is almost 0.5 V less than the maximum voltage shown in Fig. 3c. Fig. 3c shows the influence of the capacitance on both final voltage and stored charge in the capacitors after 40 s. For the small capacitor, the voltage on the capacitor is almost equal to the saturation

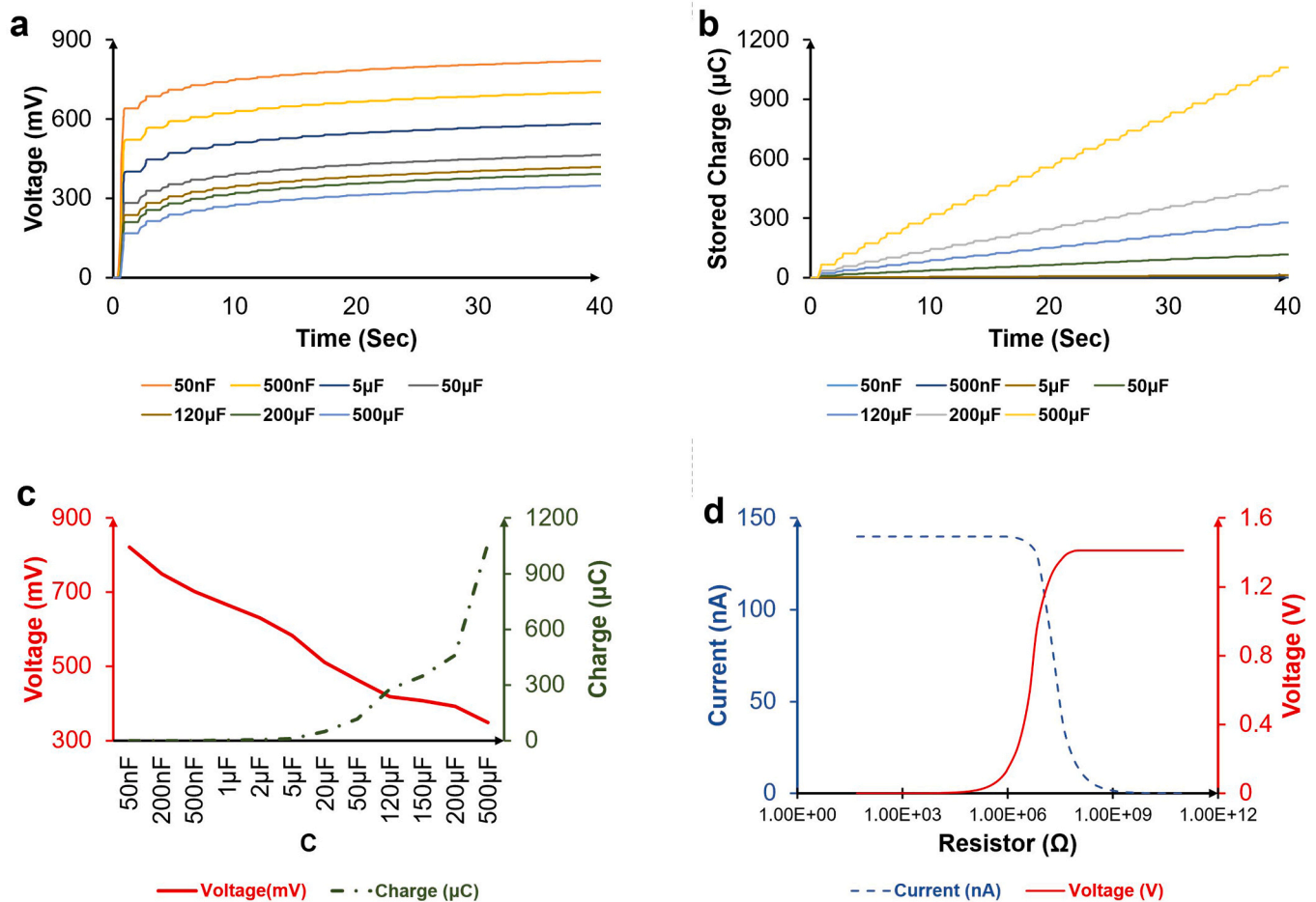


Fig. 4. SCMM charging characteristics under periodic mechanical motion. a, Voltage-time relationship at different load capacitances. b, Stored charge-time relationship at different load capacitances. c, Voltage and charge stored in the load capacitor at 40 s d, Load resistance effects on the output voltage and current.

voltage, while the stored charge, which is proportional to capacitance, is close to zero. By increasing the capacitance, the stored charge increases and the voltage decreases. Fig. 3d shows the voltage and current output for different load resistances. When the resistance is low enough (less than 100 M Ω), the current is at its peak value and the voltage is at its minimum level. When the resistance value is large enough (more than 1 G Ω in this study), the voltage is almost at its peak value and the current is close to zero.

However, the results reveal the feasibility of creating composite multifunctional mechanical metamaterial systems with sensing and energy harvesting functionalities via introducing the contact electrification into the fabrication process. It is possible to measure the force/pressure applied to the metamaterial structure by monitoring the generated voltage. The kinetic energy harvested from the external excitations by the nanogenerator metamaterial prototype can be stored for self-powering or empowering other sensing devices. Furthermore, the study reveals that we can create mechanical metamaterials whose both mechanical and electrical responses can be programmed. The snapping mechanism or the layered design of the composite matrix of the tested structure can be engineered to deform in specified order or prevent random snapping, which will result in programmed triboelectrification and mechanical behaviors. Accordingly, the SCMM concept can be applied to design a variety of programmable mechanical metamaterials with sensing, energy harvesting properties.

Furthermore, to highlight the broad real-life applications of the proposed SCMM concept, we focus on designing multifunctional automotive/aerospace engineering and biomedical systems. Here, we perform topology analysis to develop a series of multifunctional 3D hierarchical configurations based on the investigation of aforementioned

2D self-recovering SCMM designs. The first application is designing self-sensing shock absorbers with energy harvesting capabilities. The second application focuses on developing medical stents, and in particular, smart esophageal and cardiovascular stents. Figs. 5a,b and 6a,b present the mechanism and fabrication process of two SCMM-based 3D cylindrical designs for the shock absorber and stents, respectively. As seen, the 3D metamaterials can be identified as hierarchical tubes composed of 2D parallel U-shaped snapping segments at the microlevel. The esophageal and cardiovascular stents were first fabricated as auxetic SCMM films and were then configured into tubular stent form. Experimental studies were performed for further evaluation of the electrical performance of the designed 3D configurations.

Figs. 5c,d, 6c,d and 5e,f present a typical time-history response of the proposed SCMM shock absorber, esophageal and cardiovascular stents to cyclic loading at 0.1 Hz, 1 Hz and 0.05 Hz, respectively. The presented designs are proof-of-concept and are not optimized for best electrical and mechanical performance. However, incorporating the SCMM concept into the design of the shock absorber enables continuous measurement of the applied forces and harvesting the energy from the external mechanical excitations. These features are particularly important for designing advanced medical stents. Millions of cardiovascular stents are implanted every year because of their clinical efficacy. The presence of a stent within an artery can lead to excess growth of arterial tissue that may cause re-narrowing within the stent. This complication known as in-stent restenosis can reach as high as 50% among stented patients [34]. There is currently a serious need for a rapid, noninvasive, and easily accessible method to detect in-stent restenosis. A self-sensing, biocompatible and non-toxic SCMM stent equipped with a miniaturized wireless interface self-powers itself by harvesting the energy from the

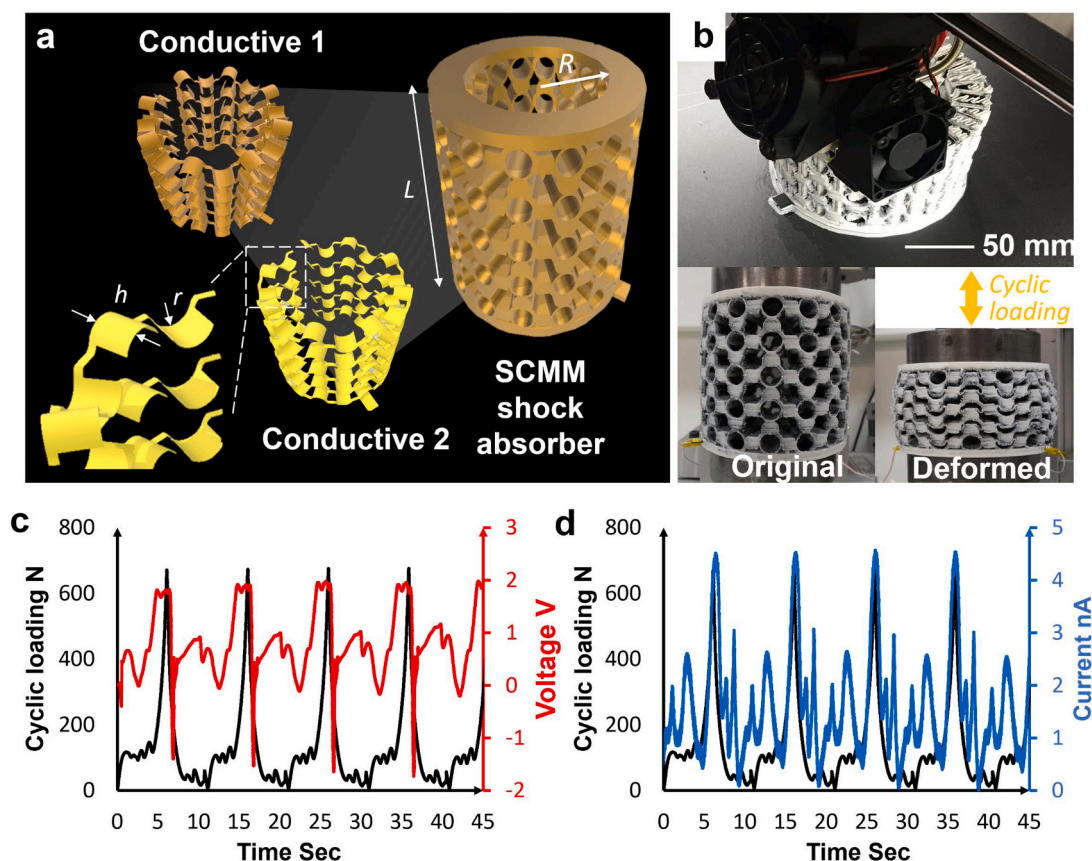


Fig. 5. Multifunctional 3D shock absorber designed based on the SCMM concept. a, Composite matrix of conductive and non-conductive layers in the SCMM shock absorber. b, 3D printing of the SCMM shock absorber prototype comprised of 80 unit cells under loading, and the shock absorber specimen at the original and deformed states under the cyclic loading. Applied cyclic loading and the corresponding c voltage (in red) and d current (in blue) signals generated by the proposed SCMM shock absorber.

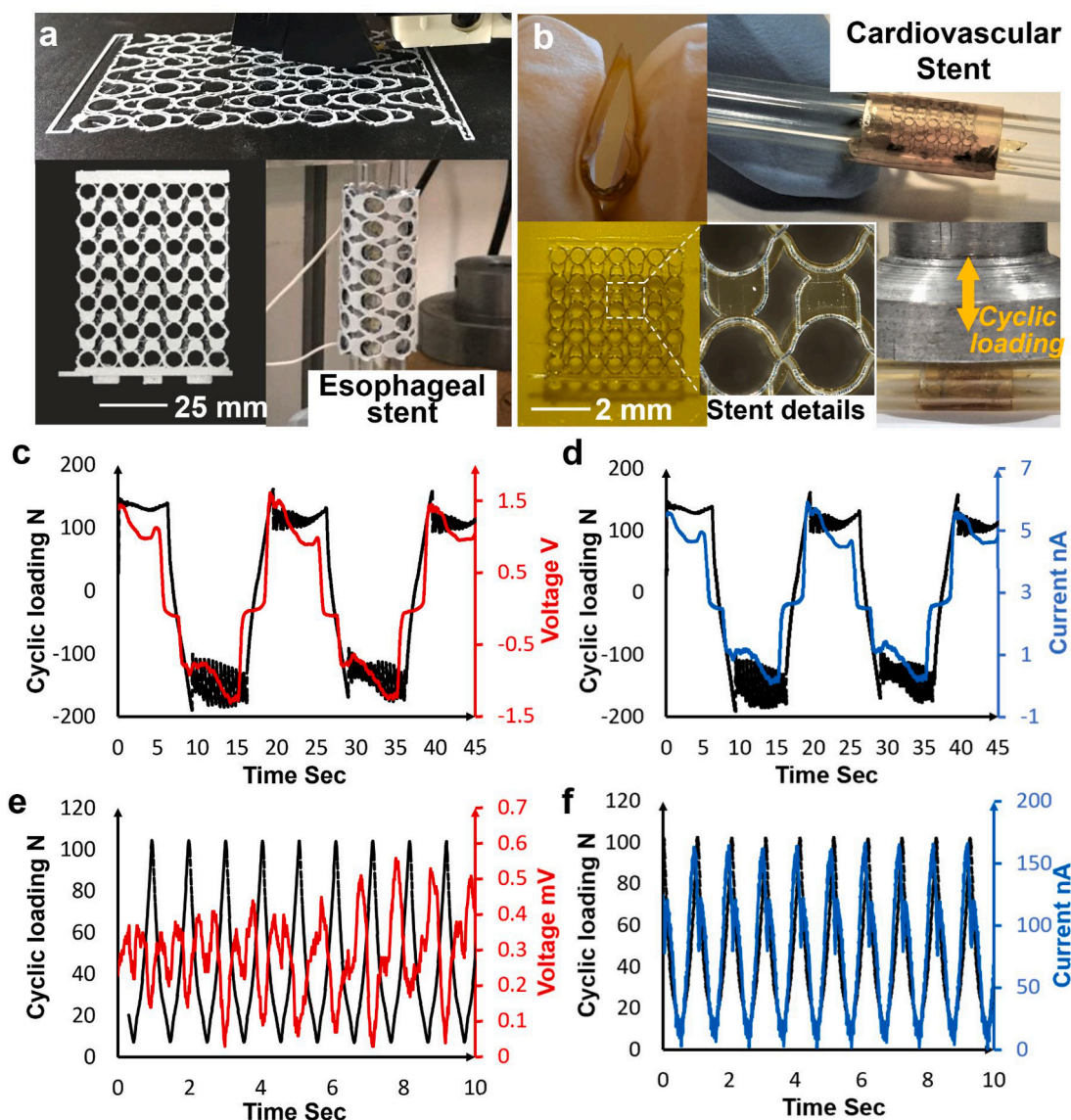


Fig. 6. Multifunctional tubular 3D stents designed based on the SCMM concept. a, 3D printing the composite matrix of the conductive and non-conductive layers in the esophageal stent prototype. b, Design details and testing of the cardiovascular stent film comprised of 5×7 unit cells. Applied cyclic loading and the corresponding c voltage and d current signals generated by the esophageal stent, and e voltage and f current signals generated by the cardiovascular stent.

arterial pulsations of the blood vessels. The stent can be deployed using a commercial balloon dilatational catheter for continuous monitoring of local hemodynamic changes upon tissue overgrowth and artery re-narrowing condition. Arguably, the same SCMM-based approach can be used to design self-powered diagnostic implants for pressure measurement in hollow internal organs and specifically esophagus, where nearby tissue grows around the stent and changes the esophagus radial pressure [35,36]. An esophageal SCMM stent empowers itself by harvesting the energy from contraction and relaxation of esophagus wall.

3. Conclusion

In summary, we proposed a new generation of meta-tribomaterial nanogenerators with energy harvesting and sensing functionalities. We leveraged advances in metamaterial design and energy harvesting to engineer new aspects of intelligence into the texture of materials for multifunctional applications. The so-called SCMM systems are fabricated using finely tailored and topologically different triboelectric microstructures. Experiments and theoretical analyses were conducted to quantitatively investigate and maneuver the mechanical and electrical

behaviors of the SCMMs. We highlighted the wide application of the proposed SCMM concept for designing proof-of-concept multifunctional material systems such as self-sensing, self-monitoring and self-powering medical stents and shock absorbers. This study opens avenue for the march toward the next stage of the technological revolution in material science in which “self-aware engineered materials and structures” can empower, sense and program themselves using their constituent components. Such SCMM systems serve as a sensing medium to directly infer multiple types of hidden information relating to the structure. Although we presented proof-of-concepts SCMMs with snapping segments, the proposed concept can be applied to many other material types with different geometrical designs. In addition to its numerous applications in the aerospace (morphing/deployable space structures) and biomedical devices (medical implants, stents, artificial muscles) areas, the proposed concept has the potential to transform the civil infrastructure and construction fields. For instance, traditional structural health monitoring approaches use dedicated sensors which often results in dense and heterogeneous sensing systems that are difficult to install and maintain in large-scale structures [37]. On the other hand, it is not always possible embed a traditional sensor (such as a strain gauge) inside structures such

as, in which cross-sectional or interlaminar failures may not be observable at the surface [38]. Another bottleneck limiting the structural health monitoring applications is that permanent monitoring systems often require extensive maintenance as a consequence of the limited durability of traditional sensors and of the limited robustness and exposure to failures of typical structural health monitoring architectures. The SCMM concept can address most of these challenges because it is a paradigm shift in technology where structure can be a sensing medium itself through a rational architectural design and choice of constituent materials. However, the novelty of the proposed concept makes it difficult to address all possible issues related to the robustness, durability or practicality of the SCMMs in actual implementation. For example, design optimization of the SCMM-based systems, optimization of the triboelectric charge density, power management and storage, and effect of fatigue on the hierarchical structures should be taken into account. Besides, there are concerns about the long-term durability of TENG-based mechanisms. To cope with this issue, it is possible to deploy some of the successful fabrication solutions that have been previously proposed to improve the durability and output stability of the TENGs for continuous operation [39].

4. Materials and methods

4.1. Fabrication of the SCMMs at the multiscale

In this study, the SCMM snapping, shock absorber and esophageal stent prototypes were fabricated using the fused deposition modeling (FDM) 3D printing technique. Raise3D Pro2 Dual Extruder 3D Printer was used to fabricate the composite samples as one integrated unit using two conductive and non-conductive materials. The fabrication process can be divided into three steps: 1) 3D modeling of the proposed design using AutoCAD and SolidWorks, 2) 3D printing of the design using a dual extruder 3D printer, and 3) removing the supports and extra printed parts from the 3D printed object. Since all layers of the prototypes (i.e. electrodes and dielectric layers) are printed simultaneously, the 3D printed samples are ready to test immediately after finishing the printing process without a need to post-printing modifications. After several preliminary tests with various conductive and non-conductive filaments and checking the generated electrical signal, PLA and TPU were found to be optimal materials for the conductive and non-conductive layers, respectively. The non-conductive TPU layer provides sufficient flexibility in the entire system. The thickness of conductive layers within the TPU framework was ranged between 0.1.1 mm and 0.3 mm. The shock absorber height, inner diameter and outer diameter were 92 mm × 16 mm × 34 mm, respectively. The esophageal stent auxetic structure had a dimension of 72 mm × 52.6 mm × 4 mm. The inner diameter of the tubular esophageal stent was 8.73 mm. A flexible polyurethane graft was inserted into the esophageal stent for testing its electrical properties. A 3D printed fixture and shaft was used to simulate the contraction and relaxation of esophagus wall during loading.

The cardiovascular stent prototype was fabricated using a 3D direct laser writer (Nanoscribe Photonic Professional, GT) (Section 1 in Supporting Information). The SCMM stent consists of two conductive parts (E1 and E2) and one non-conductive part. Each part was printed separately in shell and Scaffold mode, which print the boundary of the structure in solid but the body in a Scaffold pattern. The whole structure had a dimension of 7.5 mm × 7.5 mm × 300 μm, and were split into blocks of 220 μm × 220 μm × 200 μm, with a stitching overlap of 4 μm. The laser power was set to 90 mW, writing speed of 11 cm s⁻¹, slicing distance of 1 μm. After printing, the structures were developed in propylene glycol monomethyl ether acetate (PGMEA) bath for 30 min followed by 5 min isopropyl alcohol (IPA) rinse. After the structures were naturally dried in the air, they were placed under UV lamp for 30 min UV light flood with 16 mW/cm² intensity, which fully cross-linked the whole structure. As the direct-printed parts were all non-conductive, parts E1 and E2 were then loaded into Denton sputter coater for a

conformal coating of 30 nm Au/Pd metal film to make them conductive. All the three parts were then placed under optical microscope for assembling. To make the assembling easier, a few droplets of IPA were sprayed onto the structures to make the parts more flexible and easier to assemble. Once assembled, the assembly was detached from the substrate and glued to a flexible substrate, following by silver paste gluing of two wires to E1 and E2 electrodes for subsequent electrical measurement. The fabricated auxetic SCMM film was then configured into tubular stent form. The cardiovascular stent was directly placed under the compressive loading cycles.

4.2. Electric measurement and characterization

A TestResources Universal Testing Machine was used to apply the cyclic uniaxial loading to the 3D printed samples. A National Instruments cDAQ-9174 chassis was used as a recording device. Also, a NI9220 module with 1 GΩ impedance was used to measure the generated voltage signals. A low-noise current amplifier (SR570, Stanford Research Systems) was used to measure the currents generated by the SCMM prototypes. A LabVIEW program was developed to control and synchronize measurements from all modules and store readings in the host computer.

4.3. Electrical characterization

In the proposed snapping SCMM, the thicknesses of the dielectric layer is d_1 , and the relative dielectric constant is ϵ_{r1} . Therefore, the equivalent thickness of the dielectric layer can be written as

$$d_0 = \frac{d_1}{\epsilon_{r1}}, \quad (1)$$

and the V - Q - x relationship is expressed as [40]:

$$V = -\frac{Q}{S\epsilon_0} [d_0 + x(t)] + \frac{\sigma x(t)}{\epsilon_0}, \quad (2)$$

where ϵ_0 , σ , $x(t)$, and S denote the vacuum permittivity, charge density at the contact surface, varying gap distance, and the effective contact area, respectively. To determine the voltage V in Eq. (2), it is necessary to obtain $x(t)$ and S . Since the cyclic compression applied to the SCMM was displacement-control, the varying gap distance was determined by the loading conditions in the experiments as

$$x(t) = \frac{\Delta(t)}{n_y}, \quad (3)$$

where $\Delta(t)$ is the cyclic displacement and n_y is the number of the cylindrical units in row. Connecting the SCMM unit with a load resistance R to form a circuit, the generated voltage V can be obtained using the Ohm's law as

$$V = R \frac{dQ}{dt}, \quad (4)$$

where Q is the charge. Substituting Eqs. (3) and (4) into Eq. (2), we have

$$\frac{dQ}{dt} = -Q\Gamma + \frac{\sigma\Delta(t)}{n_y R \epsilon_0}, \quad (5)$$

where

$$\Gamma = \frac{d_0 + x(t)}{RS\epsilon_0} = \frac{n_y d_0 + \Delta(t)}{n_y SR \epsilon_0}. \quad (6)$$

Solving the ordinary differential equation in Eq. (5) leads to:

$$Q(t) = e^{-\int \Gamma dt} \int \frac{\sigma\Delta(t)}{n_y R \epsilon_0} e^{\int \Gamma dt} dt + ce^{-\int \Gamma dt}, \quad (7)$$

where c is the integration constant that can be determined by the initial conditions. Deriving Eq. (7), the voltage can be obtained as

$$V(t) = R \frac{dQ}{dt} = -R\Gamma e^{-\int_0^t r dr} \int_0^r \frac{\sigma\Delta(\xi)}{n_y R \epsilon_0} e^{\int_0^{\xi} r dr} d\xi + \frac{\sigma\Delta(t)}{n_y \epsilon_0} - c\Gamma e^{-\int_0^t r dr}. \quad (8)$$

According to the boundary conditions, we have

$$V|_{t=0} = -\frac{Q|_{t=0}}{S\epsilon_0} \left(d_0 + \frac{\Delta|_{t=0}}{n_y} \right) + \frac{\sigma\Delta|_{t=0}}{n_y \epsilon_0} = \frac{\sigma\Delta|_{t=0}}{n_y \epsilon_0} - \frac{c}{S\epsilon_0} \left(d_0 + \frac{\Delta|_{t=0}}{n_y} \right) \quad (9)$$

and

$$Q|_{t=0} = 0, \quad (10)$$

which leads to: $c = 0$. As a consequence, Eqs. (7) and (8) can be rewritten as

$$Q(t) = e^{-\int_0^t r dr} \int_0^r \frac{\sigma\Delta(t)}{n_y R \epsilon_0} e^{\int_0^{\xi} r dr} dt, \quad (11)$$

and

$$V(t) = -R\Gamma e^{-\int_0^t r dr} \int_0^r \frac{\sigma\Delta(\xi)}{n_y R \epsilon_0} e^{\int_0^{\xi} r dr} d\xi + \frac{\sigma\Delta(t)}{n_y \epsilon_0}. \quad (12)$$

To determine the charge and voltage, it is necessary to obtain the effective contact area S in Γ .

4.4. Mechanical characterization

The deformation configuration of the SCMM unit under the axial compression can be calculated as [41]:

$$EI \left(\frac{d^4 w}{dx^4} - \frac{d^4 w_0}{dx^4} \right) + p \left(\frac{d^2 w}{dx^2} \right) = -f\delta \left(x - \frac{l}{2} \right), \quad (13)$$

where w , $w_0(x)$, p , E , I , f , δ , and l are the deflection of the beam, the initial shape of the beam, the compression force of the beam, the Young's modulus, the area moment of inertia of the beam, the transverse force, the Dirac delta function, and the total length of the beam, respectively. The boundary conditions are:

$$\left\{ \begin{array}{l} w_0(x) = \frac{h}{2} W_1(x) \\ W_1(x) = 1 - \cos\left[\frac{2\pi x}{l}\right] \end{array} \right\}, \quad (14)$$

where h is the maximum height of the initial beam (i.e., radius of the SCMM unit). The general solution can be written as

$$w(x) = \sum_{i=1}^{\infty} A_i W_i(x), \quad (15)$$

where the symmetric buckling mode is:

$$\left\{ \begin{array}{l} W_i(x) = 1 - \cos\left[\frac{N_i x}{l}\right] \\ N_i = (i+1)\pi \end{array} \right\}, \quad i = 1, 3, 5, \dots \quad (16)$$

the antisymmetric buckling mode is:

$$\left\{ \begin{array}{l} W_i(x) = 1 - 2\frac{x}{l} \cos\left(\frac{N_i x}{l}\right) + \frac{2}{N_i} \sin\left[\frac{N_i x}{l}\right] \\ N_i = 2.86\pi, \quad 4.92\pi, \dots \end{array} \right\}, \quad i = 2, 4, 6, \dots \quad (17)$$

and A_i are the weight coefficients that determine the contribution of each buckling mode to the shape function. Note that A_i can be solved using the variational method⁴⁷ or the energy method⁴⁸.

The effective contact area S in Eqs. (11) and (12) are obtained as (Section 2 in Supporting Information)

$$S = \varphi \cdot 2\pi h \cdot B, \quad (18)$$

where B is the width of the electrode and dielectric layers in the SCMM. φ is the contact-separation factor give as

$$\varphi = \frac{h_{II}}{2h} = \frac{1}{6}, \quad (19)$$

where h_{II} is the radius of the cylindrical units in the buckling region (i.e., unstable). Taking Eq. (19) into Eq. (18), the effective contact area yields

$$S = \frac{1}{3} \pi h B. \quad (20)$$

Finally, substituting Eq. (20) into Eqs. (11) and (12), the total charge and voltage of the SCMM can be calculated as

$$Q_{\text{total}} = n_x n_y Q(t) \quad (21)$$

and

$$V_{\text{total}} = n_x n_y V(t). \quad (22)$$

The comparison of the output voltages between the theoretical and experimental results are provided in Section 2 in Supporting information.

Author contributions

The principal investigator is A.H.A who has conceived the SCMM concept. K.B., Q.Z., A.H.A. and Z.L.W. conceived the experiments. K.B. and Q.Z. carried out the design and fabrication supervised by A.H.A. K.B. and P.J. performed the theoretical study. K.B. and Q.Z. performed the experiments. K.B., Q.Z., A.H.A., Z.L.W. and P.J. analyzed and interpreted the data. A.H.A., K.B. and P.J. wrote the manuscript draft and all the authors discussed the results and contributed to writing portions of the manuscript and editing the manuscript. K.B., Q.Z. and P.J. contributed equally to this work.

Declaration of Competing Interest

The authors declare that they have no known competing financial interests or personal relationships that could have appeared to influence the work reported in this paper.

Data Availability

The data that support the plots within this paper and other findings of this study are available from the corresponding author on reasonable request.

Acknowledgements

Research reported in this work is supported in part by the National Institutes of Health (NIH) under award number R21AR075242-01. This research is a continuation of U.S. Provisional Pat. Ser. No. 63/048943, entitled "Self-Sensing and Self-Charging Multifunctional Metamaterials", filed on July 7, 2020 and supported by the startup funds from the Swanson School of Engineering at the University of Pittsburgh.

Appendix A. Supporting information

Supplementary data associated with this article can be found in the online version at doi:10.1016/j.nanoen.2021.106074.

References

- J.P. Lynch, K.J. Loh, A summary review of wireless sensors and sensor networks for structural health monitoring, *Shock Vib. Dig.* 38 (2) (2006) 91–128.

- [2] R.A. Swartz, J.P. Lynch, S. Zerbst, B. Sweetman, R. Rolfes, Structural monitoring of wind turbines using wireless sensor networks, *Smart Struct. Syst.* 6 (3) (2010) 183–196.
- [3] G. Park, T. Rosing, M.D. Todd, C.R. Farrar, W. Hodgkiss, Energy harvesting for structural health monitoring sensor networks, *ASCE J. Infrastruct. Syst.* 14 (1) (2008) 64–79.
- [4] Z. Chen, B. Guo, Y. Yang, C. Cheng, Metamaterials-based enhanced energy harvesting: a review, *Phys. B: Condens. Matter* 438 (2014) 1–8.
- [5] F. Cottone, H. Vocca, L. Gammaitoni, Nonlinear energy harvesting, *Phys. Rev. Lett.* 102 (2009), 080601.
- [6] S. Gonella, A. To, W.K. Liu, Interplay between photonic bandgaps and piezoelectric microstructures for energy harvesting, *J. Mech. Phys. Solids* 57 (2009) 621–633.
- [7] P. Jiao, A.H. Alavi, Artificial intelligence-enabled smart mechanical metamaterials: advent and future trends, *Int. Mater. Rev.* (2020) 1–29.
- [8] P. Jiao, H. Hasni, N. Lajnef, A.H. Alavi, Mechanical metamaterial piezoelectric nanogenerator (MM-PENG): design principle, modeling and performance, *Mater. Des.* 187 (2020), 108214.
- [9] P. Jiao, S.M. Nicaise, C. Lin, P.K. Purohit, I. Bargatin, Extremely sharp bending and recoverability of nanoscale plates with honeycomb corrugation, *Phys. Rev. Appl.* 11 (2019), 034055.
- [10] T.A. Schaedler, W.B. Carter, Architected cellular materials, *Annu. Rev. Mater. Res.* 46 (1) (2016) 187–210.
- [11] Z.G. Nicolaou, A.E. Mottter, Mechanical metamaterials with negative compressibility transitions, *Nat. Mater.* 11 (2012) 608–613.
- [12] J. Qu, M. Kadic, A. Naber, M. Wegener, Micro-structured two-component 3D metamaterials with negative thermal-expansion coefficient from positive constituents, *Sci. Rep.* 7 (2017) 40643.
- [13] K. Bertoldi, P.M. Reis, S. Willshaw, T. Mullin, Negative Poisson's ratio behavior induced by an elastic instability, *Adv. Mater.* 22 (2010) 361–366.
- [14] J.N. Grima, S. Winczewski, L. Mizzi, M.C. Grech, R. Cauchi, R. Gatt, D. Attard, K. W. Wojciechowski, J. Rybicki, Tailoring graphene to achieve negative Poisson's ratio properties, *Adv. Mater.* 27 (2015) 1455–1459.
- [15] E.B. Duoss, T.H. Weisgraber, K. Hearon, C. Zhu, W. Small, T.R. Metz, J.J. Vericella, H.D. Barth, J.D. Kuntz, R.S. Maxwell, C.M. Spadaccini, T.S. Wilson, Three-dimensional printing of elastomeric, cellular architectures with negative stiffness, *Adv. Func. Mater.* 24 (2014) 4905–4913.
- [16] T.A. Hewage, K.L. Alderson, A. Alderson, F. Scarpa, Double-negative mechanical metamaterials displaying simultaneous negative stiffness and negative Poisson's ratio properties, *Adv. Mater.* 28 (2016) 10323–10332.
- [17] X. Zheng, H. Lee, T.H. Weisgraber, M. Shusteff, J. DeOtte, E.B. Duoss, J.D. Kuntz, M.M. Biener, Q. Ge, J.A. Jackson, S.O. Kucheyev, N.X. Fang, C.M. Spadaccini, Ultralight, ultrastiff mechanical metamaterials, *Science* 344 (2014) 1373–1377.
- [18] M. Kadic, T. Buckmann, N. Stenger, M. Thiel, M. Wegener, On the practicability of pentamode mechanical metamaterials, *Appl. Phys. Lett.* 100 (2012), 191901.
- [19] X. Yu, J. Zhou, H. Liang, Z. Jiang, L. Wu, Mechanical metamaterials associated with stiffness, rigidity and compressibility: a brief review, *Prog. Mater. Sci.* 94 (2018) 114–173.
- [20] L.R. Meza, A.J. Zelhofer, N. Clarke, A.J. Mateos, D.M. Kochmann, J.R. Greer, Resilient 3D hierarchical architected metamaterials, *Proc. Nat. Acad. Sci.* 112 (37) (2015) 11502–11507.
- [21] P. Jiao, A.H. Alavi, Size-dependent buckling instability and recovery of beam-like, architected microstructures, *Mater. Des.* 162 (2019) 405–417.
- [22] B. Florijn, C. Coulais, M. van Hecke, Programmable mechanical metamaterials, *Phys. Rev. Lett.* 113 (2014), 175503.
- [23] A.A. Zadpoor, Mechanical meta-materials, *Mater. Horiz.* 3 (2016) 371–381.
- [24] Y. Li, E. Baker, T. Reissman, C. Sun, W.K. Liu, Design of mechanical metamaterials for simultaneous vibration isolation and energy harvesting, *Appl. Phys. Lett.* 111 (2017), 251903.
- [25] H. Tao, J. Gibert, Multifunctional mechanical metamaterials with embedded triboelectric nanogenerators, *Adv. Funct. Mater.* 30 (23) (2020), 2001720.
- [26] B. Deng, R. Xu, K. Zhao, Y. Lu, S. Ganguli, G.J. Cheng, Composite bending-dominated hollow nanolattices: a stiff, cyclable mechanical metamaterial, *Mater. Today* 21 (5) (2018) 467–474.
- [27] J. Chen, Y. Huang, N. Zhang, H. Zou, R. Liu, C. Tao, X. Fan, Z.L. Wang, Micro-cable structured textile for simultaneously harvesting solar and mechanical energy, *Nat. Energy* 1 (2016) 16138.
- [28] C. Jiang, C. Wu, X. Li, Y. Yao, Y. Lan, F. Zhao, Z. Ye, Y. Ying, All-electrospun flexible triboelectric nanogenerator based on metallic MXene nanosheets, *Nano Energy* 59 (2019) 268–276.
- [29] X. Li, C. Jiang, Y. Ying, J. Ping, Biotriboelectric nanogenerators: materials, structures, and applications, *Adv. Energy Mater.* 10 (44) (2020), 2002001 article 2002001.
- [30] N.I. Zheludev, The road ahead for metamaterials, *Science* 328 (2010) 582–583.
- [31] Y. Jiang, Z. Liu, N. Matsuhsa, D. Qi, W.R. Leow, H. Yang, J. Yu, G. Chen, Y. Liu, C. Wan, Auxetic mechanical metamaterials to enhance sensitivity of stretchable strain sensors, *Adv. Mater.* 30 (2018), 1706589.
- [32] G. Chen, Y. Cui, X. Chen, Proactively modulating mechanical behaviors of materials at multiscale for mechano-adaptable devices, *Chem. Soc. Rev.* 48 (2019) 1434–1447.
- [33] E. Munch, M.E. Launey, D.H. Alsem, E. Saiz, A.P. Tomsia, R.O. Ritchie, Tough, bio-inspired hybrid materials, *Science* 322 (5907) (2008) 1516–1520.
- [34] X. Chen, B. Assadsangabi, Y. Hsiang, K. Takahata, Enabling angioplasty-ready “Smart” stents to detect in-stent restenosis and occlusion, *Adv. Sci.* 5 (5) (2018), 1700560.
- [35] P. Hindy, J. Hong, Y. Lam-Tsai, F. Gress, A comprehensive review of esophageal stents, *Gastroenterol. Hepatol.* 8 (8) (2012) 526–534.
- [36] Y.K. Kim, J. Tsauo, H.Y. Song, J.H. Park, E.J. Jun, W.Z. Zhou, M.T. Kim, Evaluation of the new esophageal stent for the treatment of malignant and benign esophageal strictures, *Cardiovasc. Interv. Radiol.* 40 (2017) 1576–1585.
- [37] A.H. Alavi, H. Hasni, N. Lajnef, K. Chatti, F. Faridazar, An intelligent structural damage detection approach based on self-powered wireless sensor data, *Autom. Constr.* 62 (2016) 24–44.
- [38] R. Seifert, M. Patil, G. Seidel, Topology optimization of self-sensing nanocomposite structures with designed boundary conditions, *Smart Mater. Struct.* 28 (7) (2019), 074006.
- [39] Z. Lin, B. Zhang, H. Zou, Z. Wu, H. Guo, Y. Zhang, J. Yang, Z.L. Wang, Rationally designed rotation triboelectric nanogenerators with much extended lifetime and durability, *Nano Energy* 68 (2020), 104378.
- [40] H. Zhang, L. Quan, Electrostatic discharge - from electrical breakdown in micro-gaps to nano-generators, in: S. Voldman (Ed.), *Theoretical Prediction and Optimization Approach to Triboelectric Nanogenerator*, IntechOpen Limited, 2019, <https://doi.org/10.5772/intechopen.86992>.
- [41] K. Che, C. Yuan, J. Wu, H. Qi, J. Meaud, Three-dimensional-printed multistable mechanical metamaterials with a deterministic deformation sequence, *J. Appl. Mech.* 84 (2017), 011004.